Studies of the high field anomalous losses in small and large grain niobium cavities*

A. Romanenko[†], G. Eremeev, D. Meidlinger, H. Padamsee,
CLASSE, Cornell University, Ithaca, NY 14853, USA

Abstract

High field Q-slope in niobium cavities of all grain sizes remains to be an unexplained phenomenon. Thermometry studies performed in recent years revealed that distribution of losses in the high field Q-slope regime is not uniform, but exhibit a patchy character with some regions being hotter than other. Results of surface analysis of samples dissected from "hot" and "cold" regions of small and large BCP cavities are reported in this contribution.

INTRODUCTION

Performance of superconducting niobium cavities at high surface magnetic fields is characterized by the appearance of the high-field Q-slope effect, which is a drastic drop in the cavity quality factor at peak surface magnetic fields higher than approximately 100 mT. Several mechanisms, which were suggested as possible explanations of the effect, appeared to be either not relevant to the high field behavior or could not explain some of the established experimental facts. Since RF field penetration depth into superconducting niobium is of order 20 nm, cavity surface preparation plays a major role in the observed behavior. Baking at temperatures of 100-120°C for about 48 hours was shown to consistently remove the high-field Q-slope in EP cavities and either improve or remove it completely in BCP cavities. In most previous studies the approach used was to prepare samples in the same way as cavities and apply surface analytical techniques on them. In our work we utilize a different approach, which is:

- Prepare 1.5 GHz large and small grain niobium cavities with BCP
- Test cavities with the temperature mapping system attached
- Identify and cut out samples from cavity wall regions, which exhibited stronger (*hot*) and weaker (*cold*) heating in the high field Q-slope regime
- Analyze the samples with electron back-scattered diffraction (EBSD), X-ray photoelectron spectroscopy (XPS), Auger electron spectroscopy (AES) and optical profilometry

This method provides us with the unique opportunity to directly correlate sample properties with the high field Q-slope behavior. In this work we present results on the samples cut from small and large grain BCP cavities.

* Work supported by NSF
[†] e-mail: osr2@cornell.edu

SMALL GRAIN CAVITY

A small (≈ 1 mm) grain niobium cavity was treated with BCP for 100 μm material removal and tested with the temperature mapping system attached. In Fig. 1 the obtained Q_0 vs. E_{peak} curve is shown.

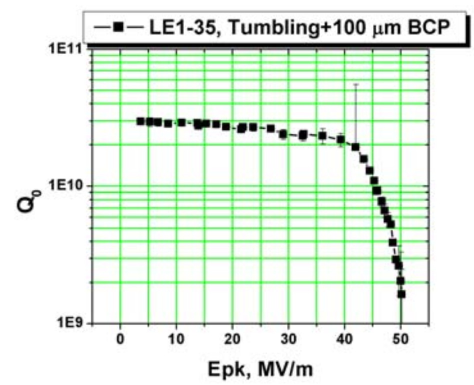

Figure 1: Q_0 vs. E_{peak} curve for a BCP-treated small grain cavity used in the experiment.

As it can be seen there was a high field Q-slope present with the onset field E_{peak} of about 40 MV/m. Temperature map was obtained at the highest field of E_{peak} = 50 MV/m, which corresponds to the peak surface magnetic field of H_{peak} = 123 mT. The maximum field reached was limited by the available power. Temperature map as obtained at the highest field is shown in Fig. 2. 12 hot and 11 cold samples covering two thermometers each were cut out from the regions with stronger and weaker heating respectively.

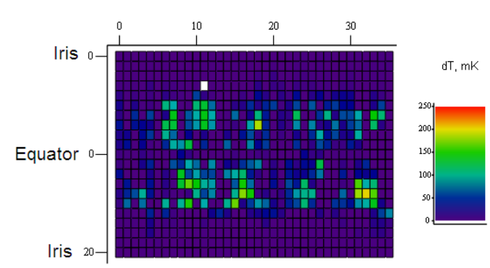

Figure 2: Temperature map at H_{peak} = 123 mT.

Typical temperature vs. field curves for hot and cold regions are shown in Fig. 3. It should be emphasized that both hot and cold regions had a high field Q-slope as can be seen from the changing of the curve slope. In fact all thermometers in the high magnetic field region indicated the high field Q-slope presence, but the amount of heating was different.

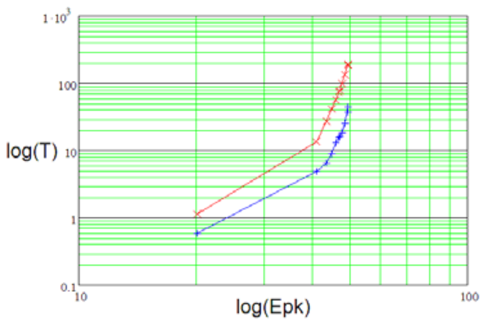

Figure 3: Typical log(T) vs. log(E_{peak}) dependence for hot (red) and cold (blue) regions.

Following subsections present results of different surface analytical techniques applied on the samples in order to study possible causes of the heating non-uniformity.

Roughness

In order to compare the roughness of hot and cold regions an optical profilometer was used. One should distinguish between the roughness observed on the micro scale at observation scale smaller than a grain size and the macro-roughness at the scale of a few grain sizes. In Fig. 4 the typical 3D profiles obtained for a hot and a cold sample are shown. From statistical analysis of the data obtained it was found that the micro-roughness for both hot and cold samples was of order σ = 1.5-2 μm.

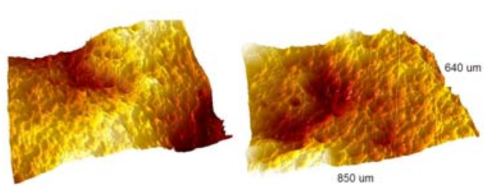

Figure 4: Optical profilometry 3-D images (850 μm $\times$ 640 μm) of the hot (left) and cold (right) samples.

The number and height of the relatively large steps due to surface irregularities such as grain boundaries is also important since they result in the magnetic field enhancement as was shown in [2]. Several line profiles were taken across a few mm of each sample surface and the histogram of a step height distribution, which is shown in Fig. 5 was constructed. As it can be seen the distributions for hot and cold samples look strikingly similar.

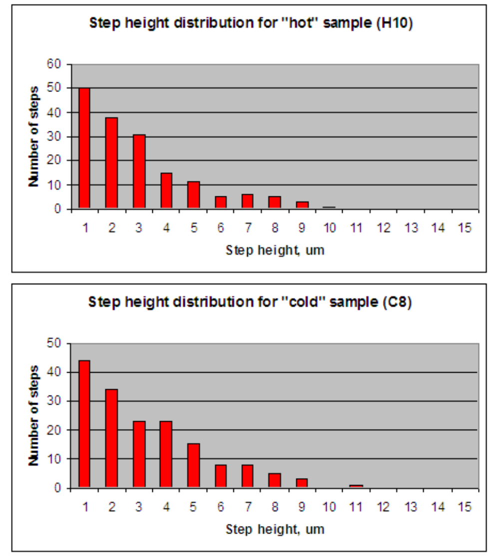

Figure 5: Step height distributions for a hot and a cold (cold) sample.

Crystalline orientation

EBSD technique was applied on the samples to obtain the crystalline orientation maps of the surface. The goal was to see if the crystalline orientation played any role in the high field Q-slope behavior of niobium. From the analysis of the data it was found that no correlation between the two existed.

Oxide structure and contaminants

Al Kα 1486.6 eV lab XPS was used for the measurements. For niobium this energy translates into information depth of about 7 nm.

Main difference, which was discovered between the hot and cold samples, was that 3 hottest out of 10 hot samples had a nitrogen signal at the level of 3-4 atomic percent present in the photoemission spectra as compared to only one spot with nitrogen signal on one of the cold samples. Fig. 6 shows typical XPS survey spectra of the samples.

Corresponding high resolution spectra around nitrogen peak are shown in Fig. 7. N 1s peak positioned at 401 eV instead of 397 eV for free nitrogen indicates that nitrogen is in the chemically bound state. One of the possible explanations for this chemical shift is that nitrogen is in the NO_3 group [1].

Mild baking of the hot sample resulted in the elimination of nitrogen signal. Since the diffusion coefficient of N in bulk Nb is too small to explain N disappearance the possible mechanism is that N diffused away along grain boundaries.

Nb 3d XPS peak, which reveals information about the oxide and oxide/metal interface, was found to be almost exactly same for all hot and cold samples analyzed as shown in Fig. 8.

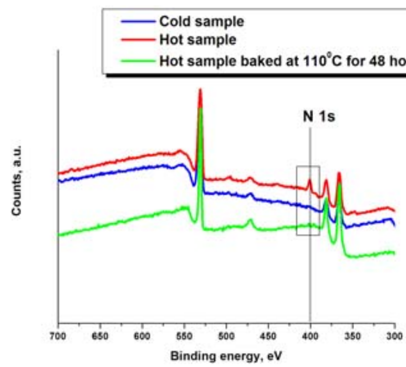

Figure 6: XPS surveys for the hot and cold samples. Hot sample was baked at 110°C for 48 hours to see the effect of baking on nitrogen.

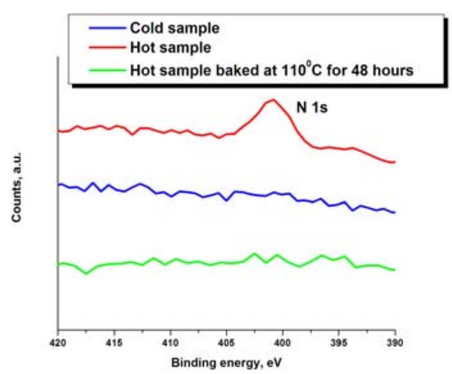

Figure 7: High resolution XPS N 1s peak for hot and cold samples.

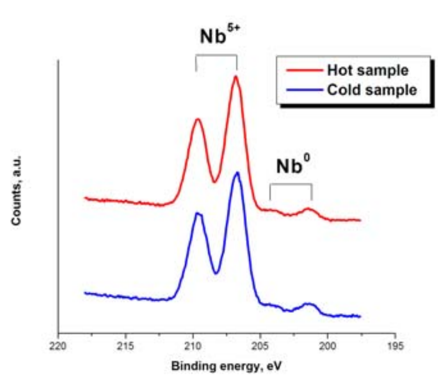

Figure 8: High resolution XPS Nb 3d peak for hot and cold samples.

In order to get a higher energy resolution and to look deeper in niobium NSLS synchrotron source with X-ray energy of 2139 eV was used for measurements on a hot and a cold sample. Results by J. Woicik are shown in Fig. 9.

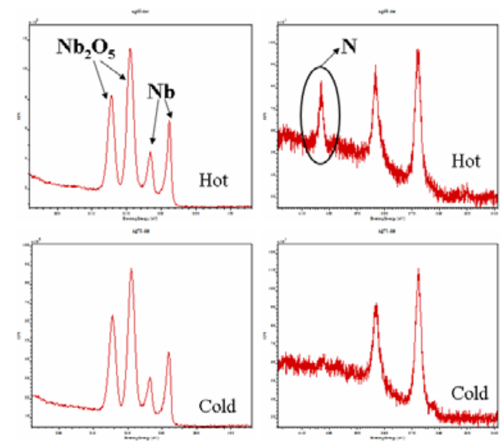

Figure 9: Nb 3d and N 1s peaks for hot and cold samples (measurements by J. Woicik).

The data confirmed results of the lab XPS, namely no difference in the oxide structure and nitrogen signal presence in the hot sample with no nitrogen in the cold one.

AES was used as a complimentary technique to confirm the presence of nitrogen. Information depth of AES for niobium is about 1 nm thus making it more sensitive to the very surface contamination and inferior to XPS for the investigation of samples. Nevertheless AES was able to detect a higher nitrogen content in the samples where nitrogen was previously found with XPS.

LARGE GRAIN CAVITY

Niobium cavity with grains of 5-10 cm, which underwent BCP, was tested with the test result shown in Fig. 10.

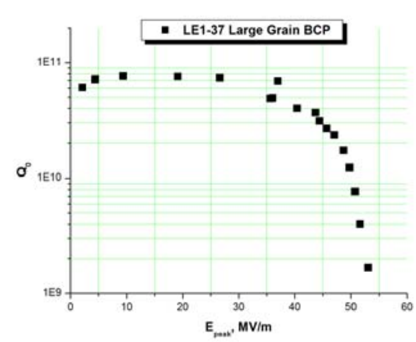

Figure 10: Q_0 vs. E_{peak} curve for a BCP-treated large grain cavity used in the experiment.

Temperature map as obtained at the highest field is shown in Fig. 11.

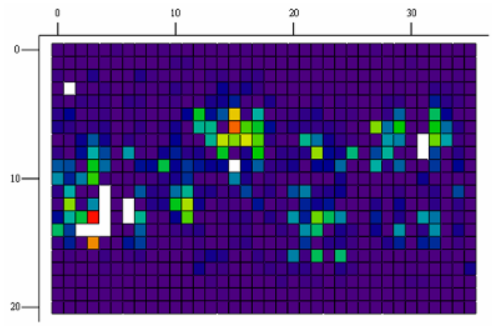

Figure 11: Temperature map at $H_{peak} \approx 120$ mT. White regions correspond to spots where temperature rise was higher than 500 mK.

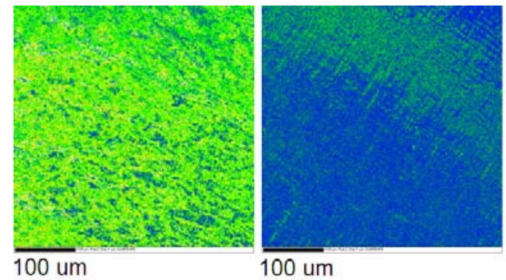

Figure 12: Local misorientation maps for "hot" (left) and "cold" (right) regions. Green color corresponds to 2° misorientation, blue - 0°.

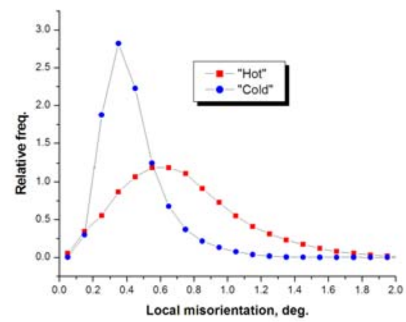

Figure 13: Local misorientation distributions as obtained from EBSD measurements.

An interesting observation is that ratio of maximum temperature rise $\Delta T_{hot}/\Delta T_{cold}$ for hot and cold regions is several times higher than in the small grain cavity. In other words, hot spots are hotter in the large grain cavity.

Twelve hot and eleven cold samples covering two thermometers each were cut out from the regions with stronger and weaker heating respectively. Following subsections present results of different surface analytical techniques applied on them.

Oxide structure and contaminants

XPS analysis of samples showed no difference in the niobium oxide structure as it was in the case of a small grain. But contrary to the small grain cavity, no excess nitrogen was found in hot regions.

Crystalline microstructure

EBSD was used for crystalline orientation mapping with a 1 μm step to get an information about the crystalline microstructure of hot and cold spots.

One of the methods of a crystalline microstructure analysis is based on a local misorientation mapping. Local misorientation is an average misorientation between the spot and its neighboring spots. It is an indirect measure of a crystal defect (i.e. vacancies, dislocations) density and distribution, which is also closely connected with strain. Though not all samples have been analyzed so far the difference was observed in the local misorientation between hot and cold regions as shown in Fig. 12- 13.

DISCUSSION

One of the main mechanisms for the high field Q-slope suggested recently was related to the possible existence of a "bad" superconducting layer underneath the natural niobium oxide (Nb_2O_5), which was thought to consist of niobium suboxides NbO and NbO_2 or a very high content of an interstitial oxygen. In our studies we did not find any difference in the oxide or oxide/metal interface in hot and cold regions. That allows to eliminate the oxide layer from possible causes of the observed heating non-uniformity.

Another theory of the high field Q-slope origin proposed in the early stages is based on the magnetic field enhancement at surface topographical irregularities (i.e. grain boundaries) [2]. Our optical profilometry studies showed that roughness was not the cause of the patchy distribution of losses in BCP cavities. Grain boundary role was also eliminated in other temperature mapping studies [3, 4].

Crystalline microstructure was not on the list of possible candidates for the Q-slope cause. But now differences observed in the local misorientation between hot and cold regions suggest that crystal defect (i.e. vacancies, dislocations) density might be the driving factor for the heating non-uniformity. At this point the full interpretation of results is not clear.

The observed correlation between the presence of nitrogen and the high field Q-slope severity in a small grain cavity suggests that nitrogen might play a role in the effect. Since nitric acid (HNO_3) is one of the components of a BCP solution it is possible that the high field Q-slope might be related to the BCP procedure. But since nitrogen was found only in the small grain cavity and no nitrogen in the large grain one it might be a secondary effect. For example, nitrogen might segregate at regions with higher crystal defect density.

CONCLUSION

Summarizing, the first attempt to directly correlate results of surface studies with the behavior of niobium at high surface magnetic fields via cutting cavities proved to be successful. Further experiments based on the same approach will be carried out in the near future.

ACKNOWLEDGMENTS

Authors want to thank J. Shu and J. Woicik for XPS analysis of some samples.

REFERENCES

[1] V. S. Chathapuram et al., Microelectronic Engineering, Volume 65, Issue 4, May 2003, pp. 478-488.

[2] J.Knobloch et al., Proc. of the 9th Workshop on RF Superconductivity, 1999, Santa Fe, USA, pp.77-91.

[3] G. Eremeev and H. Padamsee, Proceedings of the 2006 European Particle Accelerator Conference, Edinburgh, UK, MOPCH176.

[4] G. Ciovati et al., Phys. Rev. ST AB 10 (2007).